Morphology of ground states of two-dimensional frustration model

1982 J. Phys. A: Math. Gen. 15 673

(http://iopscience.iop.org/0305-4470/15/2/033)

J. Phys. A: Math. Gen. 15 (1982) 673–699. Printed in Great Britain

Morphology of ground states of two-dimensional frustration model

F Barahona†, R Maynard†, R Rammal† and J P Uhry‡

† Centre de Recherches sur les Très Basses Températures, CNRS, BP166X, 38042 Grenoble Cedex, France

‡ Recherche opérationnelle, Laboratoire IMAG associé au CNRS, Université Scientifique et Médicale de Grenoble, BP 53 X, 38041 Grenoble Cedex, France

Received 13 April 1981

Abstract. The problem of generating ground states of a quenched random Ising spin system with variable concentration of mixed-neighbour exchange couplings ($J_{ij} \lesseqgtr 0$) on a planar lattice (frustration model) is mapped into the problem of the Chinese postman which has been solved by a polynomial algorithm known as Edmond's algorithm. This algorithm is transposed and applied to the frustration problem. Not only is one particular ground state generated, but a post-optimal algorithm is established which gives the map of the rigid bonds and solidary spins (bonds in the same state for *all* ground states). This study of the rigidity on a square lattice reveals three distinct regimes by varying x, the concentration of negative bonds:

(1) a low-concentration regime where the ground states are rigid and ferromagnetic;

(2) an intermediate regime $0.1 \leqslant x \leqslant 0.15$ where the rigid ground states are structured in an antiphase domain separated by magnetic walls;

(3) a high-concentration regime where the clustering of solidary spins is finite and separated by fracture lines.

These defects characterise the phase transitions between the ferromagnetic, the random antiphase and the paramagnetic states which occur with increasing x.

1. Introduction

It is now accepted that the spin glass problem is of great difficulty and cannot be directly transposed from methods which were successful in the study of homogeneous models. As an example we mention here the great difficulty of providing ground states of spin glass systems, while these states are obtained simply in homogeneous models as well as diluted ferromagnetic models of percolation. This step in the progress of knowledge of this problem is crucial for the following reasons: the controversy between those who believe that the low-temperature properties are purely metastable, and the supporters of a phase transition towards a cooperative frozen state of spins, can evolve if one learns that the ground state does not contain any long-range correlation (as is shown in this paper for the model $\pm J$ in two dimensions at $x = 0.5$; see below). Also, the analytical calculations are of great complexity at low temperatures and, except for the solution of Parisi (1979) of the infinite-range model, very few results have been firmly settled. The description of *exact* ground states as presented in this paper could provide the inspiration for a correct solution.

0305-4470/82/020673+27$02.00

The model $\pm J$ is defined by the Hamiltonian

$$H = -\sum_{(i,j)} J_{ij}\sigma_i\sigma_j$$

where σ_i, $\sigma_j = \pm 1$ are Ising spins on a square lattice, and J_{ij} is the random interaction between nearest-neighbour spins with probability x for $J_{ij} = -J$ and $1-x$ for $J_{ij} = J$. It has been shown (Binder 1980) that this model shows most of the features of more realistic models like that with the gaussian distribution of J'_{ij}, except the residual entropy $S(0)$ which is very important in the $\pm J$ model. This corresponds to a huge degeneracy of the ground states (typically 10^{13} for a 20×20 spin at $x = 0.5$); the corresponding low-energy excited states of the gaussian model are manifest up to a temperature $T \simeq 0.3$ in J units. But it is hard to perform an exact thermal average over these low-energy excited states, since the enumeration of these states must be exhaustive; this will be done here using a polynomial algorithm exploiting entirely the symmetry of the $\pm J$ model. Then, instead of deploring this huge degeneracy of ground states, we think that the thermodynamic variables (correctly averaged over all ground states) are very representative of low-temperature properties of Ising spin glass models.

The failure of the Monte Carlo relaxation method to provide exact ground states is now well established (Bray and Moore 1977, Kirkpatrick 1977). It turns out that this relaxation process traps the system into low-energy metastable states of very long lifetime separated from the ground state by potential barriers (Rammal *et al* 1979). The other attempts to construct exact ground states are initiated by the analysis of spin configurations in terms of frustrated plaquettes (squares of spins with an odd number of negative J_{ij} on the perimeter) and strings of violated bonds (Toulouse 1977). The rules resulting from the latter methods have been applied by hand (Vannimenus and Toulouse 1977, Vannimenus *et al* 1979) on samples of finite size. The first purely computational method (Bieche *et al* 1980) used a matching method of graph theory known as the Edmonds method. The present study is very akin to this matching method: however it works on the graph of spins, bond variables and frustrated contours. This new formulation is much more transparent than the previous one and some analogy with defect theory is suggested. In § 2, the ground-state problem of the frustration model is formulated as the Chinese postman's problem, for which a dual problem is built. This dual problem uses frustrated contours which appear as the natural conjugates of the violated bonds. The principle of the solution is sketched in § 3 as well as the close analogy between the frustration problem and dislocation theory. The usefulness of this new version of this algorithm resides in the post-optimality procedure which produces the rigidity of bonds for all the ground states (a rigid bond is by definition an edge which keeps its two spins in the same relative orientation in all ground states. The spins are said to be solidary). This property is crucial for discussing the magnetic correlation between spins. Actually, spins which belong to the same cluster of rigid bonds are perfectly correlated. Conversely, spins sitting in distinct clusters are less correlated. Any long-range order will be supported by an infinite (percolating) cluster of rigid bonds.

Section 4 is more technical: it is devoted to the primal algorithm and the strategy for producing optimal solutions. It is shown that any transient solution is reached by reversing a set of spins of any shape. It is the non-local character of the transition which overcomes the potential barrier present in the system even in the low-energy excited state.

The numerical experimentation is presented in § 5. The boundary conditions are not unimportant in the present context; actually two types of boundary conditions are produced by the algorithm—periodic and antiperiodic—for the optimality. This additional degree of freedom plays an important role for the discovery of the so-called antiphase state.

The results are presented in § 6. An effort of visualisation of the morphology of the ground states has been made. It is shown how the rigidity of the ferromagnetic ground state is 'pulverised' by adding negative bonds. When the content of frustrated plaquettes is increased fracture lines occur. A threshold for disappearance of rigidity is located at $x \sim 0.15$. The structures of percolation clusters or finite clusters are indeed very different from those in the uncorrelated percolation problem, since the threshold is found at the concentration 0.7 of rigid bonds. At intermediate concentrations of negative bonds, $0.1 < x < 0.15$, a systematic choice of antiperiodic boundary conditions indicates the presence of magnetic walls in rigid ground states. The occurrence of these magnetic defects indicates here the existence of a new phase called the random antiphase state with zero magnetisation. It must be noticed that this state is highly correlated: a correlation function of the staggered magnetisation of the type $\langle S(0)\, S(R)\rangle_0^2$, where the averaging over all ground states is indicated by the brackets, has its maximum value inside the percolating cluster of rigid bonds.

In § 7, the main results of this study are summarised and a clear distinction between the two types of defects is put forward. Possible generalisations to gaussian models are also evoked.

2. The frustration model as the Chinese postman's problem

This section is devoted to the relationship between the frustration model and the Chinese postman's problem. After recalling some important definitions, we give the general formulation of the frustration problem in terms of finding a minimum weighted cut in a particular graph. For planar graphs without isthmus, there is a one-to-one correspondence between cuts and quasi-cycles of the dual graph (a quasi-cycle is an edge set such that each node has even degree). This property permits the reduction of the frustration problem to that of finding a minimum weighted quasi-cycle, which can be solved in polynomial time. Consequently, frustrated contours appear as the only pertinent variables in the frustration model and emerge naturally from our new formulation.

2.1. The Chinese postman's problem (Mei-Ko Kwan 1962)

A postman delivers mail along a set of streets represented by the edges of a connected graph G. He must go along each street at least once, in either direction. He starts at the post office (one of the nodes of G) and must return to this starting point. What route enables the postman to walk the shortest possible distance?

The problem is to find a minimum length closed path, with repeated edges if necessary, which contains each arc of a given network (figure 1).

Assume the network connected, and all edge weights (here lengths) non-negative. If the degree of each node is even, then the network is Eulerian and the solution is simply an Euler path. Such a path, which contains each edge exactly once, is certainly as short as any closed path which contains each edge at least once.

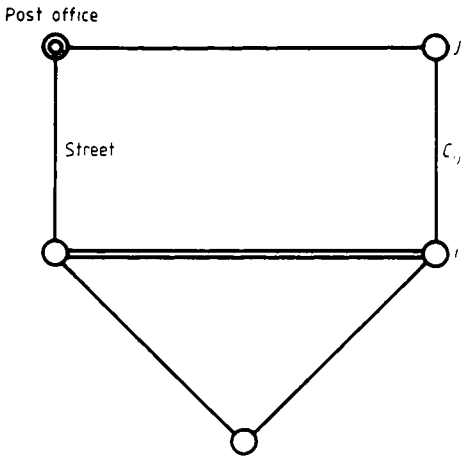

Figure 1. The Chinese postman's problem.

It is easy to see that the occurrence of odd-degree nodes (network G not Eulerian) implies repeated edges in the postman's walk (there is no Eulerian path). These observations enable us to formulate the Chinese postman's problem as follows.

Let $G = (V, E)$ be a given connected graph, with $C_{ij} > 0$ as the weight of the edge $(ij) \in E$. V' denotes the set of nodes having odd degree, $V'' = V - V'$. The problem of the Chinese postman on the weighted graph G can be formulated as the following integer linear programming problem:

(C1) minimise $\sum_{(ij)\in E} C_{ij}x_{ij}$ subject to

(C2) $\sum_{j} x_{ij} = 1 \pmod 2$ for each $i \in V'$,

(C3) $\sum_{j} x_{ij} = 0 \pmod 2$ for each $i \in V''$,

(C4) $x_{ij} \in \{0, 1\}$ for each $(ij) \in E$.

The value 1 of x_{ij} indicates the repetition of the edge (i, j) in the weight function. This problem, dubbed 'Chinese' by Edmonds in recognition of the mathematician Mei-Ko Kwan who proposed it, was solved by Edmonds by a procedure which employs the matching algorithm (Edmonds 1965, Edmonds and Johnson 1973).

2.2. The ground-state problem in the frustration model of a spin glass

In this model, on a graph $G = (V, E)$, with each mode $i \in V$, there is associated a single variable σ_i, with the possible values ± 1 indicating spin orientations (Ising model), and with each edge $(ij) \in E$ there is associated a weight $J_{ij} \in R$ indicating the interaction between spins. The ground state ($T = 0$ K) is found by minimising the corresponding energy of spins,

$$H = -\sum_{(ij)\in E} J_{ij}\sigma_i\sigma_j,$$

where $\{J_{ij}\}$ is given, i.e. maximising $\Sigma_{(ij)} J_{ij}\sigma_i\sigma_j$ subject to $\sigma_i = -1, 1$.

In the following subsections, we establish the equivalence between the two problems, as well as the correspondence dictionary.

2.3. The ground-state problem, as a minimum weighted cut problem

For a given spin configuration (an assignment of values to variables σ_i), we denote by U the set of spins up ($\sigma_i = +1$), and by D that of spins down ($\sigma_i = -1$).
Let

$$W^+ = \sum_{\substack{(ij) \\ \sigma_i = \sigma_j = 1}} J_{ij}, \qquad W^- = \sum_{\substack{(ij) \\ \sigma_i = \sigma_j = -1}} J_{ij}, \qquad W^{+-} = \sum_{\substack{(ij) \\ \sigma_i \neq \sigma_j}} J_{ij}.$$

Obviously, we have

$$-H = W^+ + W^- - W^{+-} = K - 2W^{+-}$$

where $K = W^+ + W^- + W^{+-}$ is a constant (i.e. $|E|$ if $J_{ij} = \pm 1$). Therefore, minimising H is equivalent to minimising W^{+-}. This problem is known in graph theory terminology as the problem of finding a minimum weighted cut. In the frustration problem a cut is given simply by a partition of spins (U, V) (see figure 2). It is precisely the set of edges which connects nodes of U with nodes of D.

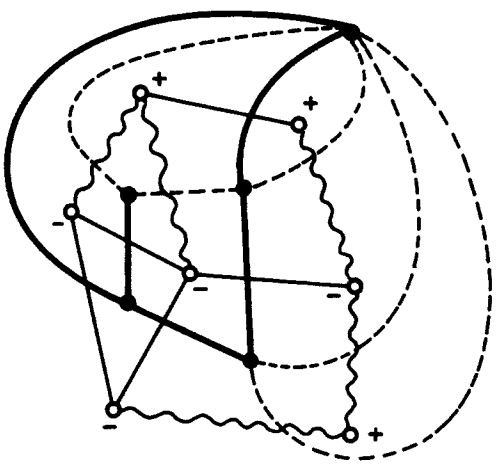

Figure 2. The wavy lines represent the cut, the broken lines the quasi-cycle.

2.4. The two-dimensional case or planar graph

In the following, we assume the planarity of the graph $G = (V, E)$ and we denote by G^* its dual graph. To each cut (U, D) corresponds a partial graph of G^*, such that each node has even degree: this partial graph is by construction the quasi-cycle associated with the considered cut (see figure 2). In Orlova and Dorfman (1972) it is shown that for planar graphs G without isthmus, there is a one-to-one correspondence between cuts and quasi-cycles of the dual graph G^*. Then, for a planar graph, the problem of finding a minimum weighted cut is equivalent to that of finding a minimum weighted quasi-cycle in the dual graph (the latter problem may be solved in polynomial time (Edmonds 1965)).

For clearness we adopt here the frustration terminology and limit our discussion to planar frustrated graphs.

Definitions

For a quasi-cycle Q, let an edge (ij) be violated if $J_{ij} > 0$ and (ij) belongs to Q, or if $J_{ij} < 0$ and (ij) does not belong to Q. An edge will not be violated otherwise.

Let

$$x_{ij}(Q) = 1 \text{ if } (ij) \text{ is violated,}$$
$$= 0 \text{ otherwise.}$$

In order to show the relationship with the Chinese postman's problem we shall establish conditions (C2), (C3) and (C1).

(C2), (C3)

It is easy to see that for a quasi-cycle there is an odd number of violated edges adjacent to odd nodes and an even number adjacent to even nodes. Thus we recover (C2), (C3) where V' is the set of frustrated plaquettes (nodes of G^* corresponding to elementary frustrated cycles†). In this way, the set of frustrated plaquettes corresponds to odd nodes in the Chinese postman's problem, and frustrated edges correspond to repeated arcs in its walk.

Objective function (C1)

In order to complete the proof, we denote by $W(Q)$ the total weight of the quasi-cycle Q, and

$$u(Q) \equiv H = W(Q) - W(E-Q) = 2W(Q) - W(E)$$

where $W(E)$ is the total weight of edges. It is easy to see the following identity:

$$u(Q) = \sum_{(ij)\,\text{violated}} J_{ij} - \sum_{(ij)\,\text{non-violated}} |J_{ij}|.$$

In fact, if $J_{ij} > 0$ and (ij) violated, then $(ij) \in Q$ and its weight in $u(Q)$ occurs as $|J_{ij}|$.

If $J_{ij} < 0$ and (ij) violated, then $(ij) \notin Q$ and its weight in $W(Q)$ occurs as $-J_{ij} = |J_{ij}|$. The same argument holds for non-violated edges. Finally, we have

$$u(Q) = K + 2 \sum_{(ij)\,\text{violated}} |J_{ij}| \qquad \text{where } K = \sum_{(ij)\in E} J_{ij}.$$

Therefore, the minimum of H is given by that of $\Sigma_{(ij)} |J_{ij}| x_{ij}$, and we recover (C1). This proof achieves the correspondence between the two problems mentioned in the introduction of this section (see table 1).

NB The correspondence: frustration problem ↔ minimum weighted cut holds in any graph. The planarity property is evoked only in the correspondence: cut ↔ quasi-cycle.

† A cycle C is said to be frustrated if $\prod_{(ij)\in C} \text{sgn}(J_{ij}) = -1$, and not frustrated otherwise.

Table 1. Correspondence dictionary: Chinese postman–frustration.

Chinese postman's problem	Frustration problem
Odd nodes	Frustrated plaquettes
Repeated edges in the walk	Frustrated edges
Additional 'cost'	Frustration energy

2.5. Reformulation of frustration problem

Using the equivalence shown above, between the frustration model and the Chinese postman's problem, we are in a position to reformulate the frustration problem in more general terms. Let $H = (X, F)$, a planar graph with a weighting function $w: F \to \mathbb{R}$. For $Q \subseteq F$, we denote by $v(Q)$ the set of violated edges;

$$F^+ = \{e \in F,\ w_e > 0\}, \qquad F^- = \{e \in F,\ w_e < 0\}.$$

A node $v \in X$ is said to be odd (even) if and only if $|\delta(v) \cap F^-|$ is odd (even). Here the cardinality $\delta(v)$ denotes the set of edges in F, adjacent to the node $v \in V$ ($|A|$ means cardinal of A). It is straightforward to show the following properties.

(i) $Q \subseteq F$ is a quasi-cycle if and only if

$$|v(Q) \cap \delta(v)| = \begin{cases} 1 & (\text{mod } 2) \text{ if } v \in X \text{ is odd,} \\ 0 & (\text{mod } 2) \text{ if } v \in X \text{ is even.} \end{cases}$$

(ii) For a quasi-cycle Q, we have

$$\sum_{e \in Q} w_e = \sum_{e \in v(Q)} |w_e| + \sum_{e \in F^-} w_e.$$

(In relation to (2.4), X represents the set of nodes in the dual graph, and w_e corresponds to the interaction J_{ij}.)

Therefore, in order to minimise the total weight of the quasi-cycle Q, we need to minimise $\Sigma_{e \in v(Q)} |w_e|$. Thus, if we denote

$$x_e = \begin{cases} 1 & \text{if } e \in v(Q), \\ 0 & \text{if } e \notin v(Q), \end{cases}$$

the ground-state problem in the frustration model can be formulated as the following integer linear programming problem (i.e. Chinese postman's): minimise $\Sigma_{e \in F} x_e |w_e|$ subject to

$$\sum_{e \in \delta(i)} x_e = 1 \ (\text{mod } 2) \text{ for } i \text{ odd},$$

$$\sum_{e \in \delta(i)} x_e = 0 \ (\text{mod } 2) \text{ for } i \text{ even}, \qquad x_e \in \{0, 1\}.$$

This linear problem can be solved in polynomial time, as shown by Edmonds and Johnson (1973) (see § 3). The main result of these authors is to rule out the integrality condition $x_e \in \{0, 1\}$ by adding new linear constraints on the set of odd subsets of H. An odd subset of H is simply a subset of X containing an odd number of odd nodes and any number of even nodes; such a subset is denoted by S.

Thus, the integer linear program above may be stated in the following way:

$$(P_0)\begin{cases}\text{minimise } \sum_e |w_e| s_e \text{ subject to} \\ \sum_{e\in\delta(S)} x_e \geqslant 1 \text{ for any odd subset } S, \qquad x_e \geqslant 0,\end{cases}$$

where $\delta(S)$ is the set of edges having exactly one end in S.

By dropping the integrality requirement, $x_e \in \{0, 1\}$, and adding the linear constraints on subsets S, we obtain a linear program whose feasible solutions include all feasible solutions of the original one. In particular, if this linear program has an integer-valued optimal solution, then that solution is optimal for the original one.

2.6. Signification of the program (P_0)

In order to understand the signification of the program (P_0) it is more useful to use the frustration terminology, which gives a transparent and intuitive picture (figure 3).

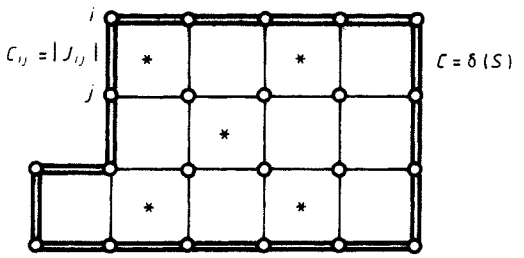

Figure 3. The * represent the frustrated plaquettes. $C = \delta(S)$ is a frustrated contour.

In the planar graph of spins, the set of odd nodes of its dual are nothing other than the set of frustrated plaquettes. An odd subset S is nothing other than a set of plaquettes having an odd number of frustrated plaquettes; finally, $\delta(S) \equiv C$ are simply the frustrated contours, delimiting naturally this odd subset with an odd number of frustrated plaquettes.

Armed with this interpretation, we obtain the *main result* of this section, by restating the ground-state problem of the frustration model as follows:

$$(P)\begin{cases}\text{minimise } \sum_{(ij)\in E} |J_{ij}| x_{ij} \text{ subject to} \\ \sum_{(ij)\in C} x_{ij} \geqslant 1 \text{ for any frustrated contour } C, & \text{(P1)} \\ x_{ij} \geqslant 0. & \text{(P2)}\end{cases}$$

The primal linear program (P) gives the following intuitive picture: a constraint on frustrated contours, C, is the simple property of the occurrence of at least one frustrated edge in a frustrated contour. This property emerges naturally from the statement above and represents the cost of replacing the integrality condition $(x_{ij} \in \{0, 1\})$ by $x_{ij} \geqslant 0$.

The program (P) evokes only the graph of spins, without any variables coming from the dual one. In this way our new formulation is more transparent than that used previously (Bieche *et al* 1980). The main feature to be noted here is the natural way in

which the set of frustrated contours emerges. In fact, this set contains the whole pertinent information of the frustration as well as the natural variables of the problem.

3. Solution of the frustration problem by duality: rigidity

In this section we shall describe the dual program of (P), and we shall give its physical content. In particular, we show the close analogy between dislocations and frustrated plaquettes, as well as frustrated contours and Volterra circuits in the defects theory of crystals. After summarising the main steps of the primal–dual solution, we shall demonstrate the usefulness of the algorithm as a post-optimality procedure, giving the rigidity of ground states. A more detailed description of the technical points will be given in the Appendix.

3.1. Dual problem (D)

In order to solve the program (P), it is usual in linear programming to introduce the dual program (D). (P) is called the 'primal' problem and (D) is its 'dual'. In the program (P), the x_{ij} are the unknown variables, and they are associated with the set of edges. In contrast, in the program (D), the unknown variables y_s are associated with frustrated contours $C = \delta(S)$.

The dual program (D) may be stated in the following way:

$$(\mathrm{D})\begin{cases} \text{maximise } \sum_s y_s \text{ subject to} \\ \sum_{\{S/(ij)\in\delta(S)=C \text{ frustrated}\}} \leqslant C_{ij} = |J_{ij}| \text{ for any } (ij)\in E, & (\mathrm{D1}) \\ y_s \geqslant 0. & (\mathrm{D2}) \end{cases}$$

The correspondence between (P) and (D) is very clear: $\{y_s\}$ is the analogue of Lagrange multipliers associated with (P1) and D1 is associated with the x_{ij}.

The variables y_s conjugated to the x_{ij} represent a repartition of frustration energy (cost) among frustrated contours (see below). The values taken by the y_s are dictated in general by those of the J_{ij}. For instance, if $J_{ij} = \pm 1$, then the y_s can belong to $\{0, \frac{1}{2}, 1\}$ for all S. More generally, if $C_{ij} = |J_{ij}|$ are integers, the y_s are half-integers ($y_s \in \frac{1}{2}\mathbb{Z}$). In the general case, to real C_{ij} correspond real y_s.

3.2. Primal–dual solution

A feasible solution of (D), i.e. a repartition $\{y\}$ satisfying (D1) and (D2), gives a lower bound for the frustration energy

$$\sum y_s \leqslant \sum |J_{ij}| x_{ij}.$$

The best lower bound, $\max \Sigma\, y_s$, yields the minimum of the frustration energy

$$\min \sum |J_{ij}| x_{ij}.$$

Therefore, if $X = \{x_{ij}\}$ is a feasible solution of (P), X is an optimal one if there exists a feasible solution $\{y\}$ of (D) such that (see figure 4)

$$\sum y_s = \sum |J_{ij}| x_{ij}.$$

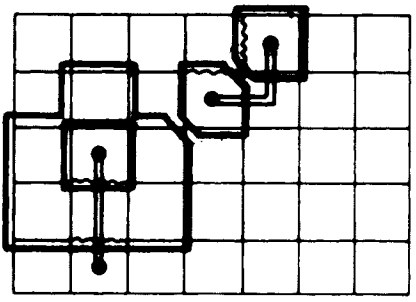

Figure 4. The straight bonds represent $J_{ij} = +1$ and the wavy bonds $J_{ij} = -1$. The violated edges correspond to the double line. The wavy lines indicate the contours S with $y_s = 1$.

The following 'complementary slackness' conditions give an optimum criterion for a pair (X, Y) of feasible solutions of (P) and (D):

(i) if $x_{ij} > 0$, then $\Sigma_{\{S;(ij)\in\delta(S)\}} y_s = C_{ij} \equiv |J_{ij}|$, S is a odd subset;

(ii) if $y_s > 0$, then $\Sigma_{(ij)\in C=\delta(S)} x_{ij} = 1$.

This criterion is the main point in the algorithm summarised below. On the other hand, we can extract immediately from (i)–(ii) some results about the rigidity of ground states. In fact:

(a) If the condition $\Sigma_{\{S;(ij)\in\delta(S)\}} y_s < |J_{ij}|$ is satisfied, then the edge (ij) cannot be frustrated in any optimal solution (i.e. any ground state). (ij) is called in this case a rigid bond.

(b) If the condition $y_s > 0$ is satisfied, then the frustrated contour $C = \delta(S)$ has exactly one frustrated edge in the whole set of ground states.

These two remarks are the starting point of the rigidity analysis given below.

3.3. Analogy with dislocations

As stated above, the variables $x_{ij} \in \{0, 1\}$ indicate the repartition of frustrated edges in the graph of spins. On the other hand, the variables y_s represent a kind of 'line tension' of frustrated contours $C = \delta(S)$ arising from the energy excess due to frustration. This observation permits us to draw a simple analogy between the frustration problem and dislocation theory in crystals.

We can see such a correspondence as follows. A frustrated plaquette is nothing other than the dislocation core, and a frustrated contour is simply the counterpart of a Volterra circuit (see figure 5).

The 'line tension' y_s represents the self-energy of a dislocation, and the analogue of the Burgers' vector is the total charge inside the frustrated contour C. The main difference between the two problems is the composition law (addition) of topological charges: $Z_2 = Z/2Z$ in the frustration problem instead of Z for dislocations.

This picture gives a new insight to the old naive idea representing a glass as a material with a high density of dislocations. In our case, we have a set of 'magnetic dislocations'.

3.4. Hierarchical structure of frustrated contours

Instead of using all odd subsets S, we can show that *connected* odd subsets of S are sufficient for our investigations. Moreover, we can limit ourselves to a family having the

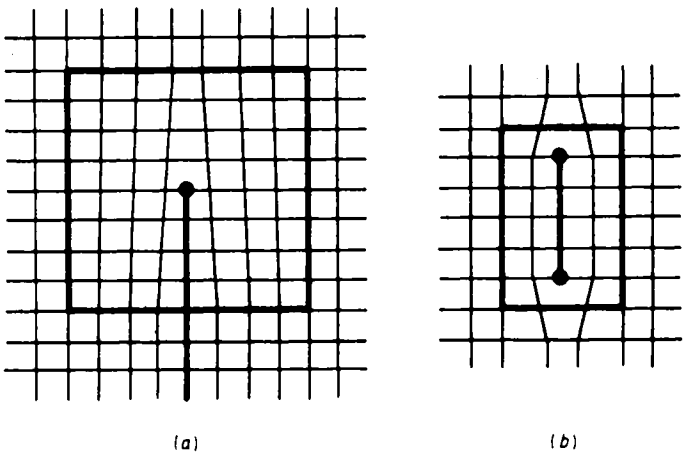

Figure 5. Analogy frustration–dislocation. (*a*) Odd subset (circuit) with odd number of charges. (*b*) Even subset (circuit) with even number of charges.

following property: for any pair $S1$, $S2$ of odd subsets we have: either $S1 \subset S2$ (respectively $S2 \subset S1$) (embedding properties) or $S1 \cap S2 = \varnothing$.

In this way, we have a *hierarchical* structure of frustrated contours S, having $y_s > 0$ (figure 6) . The physical consequence of this structure is not clear to the authors.

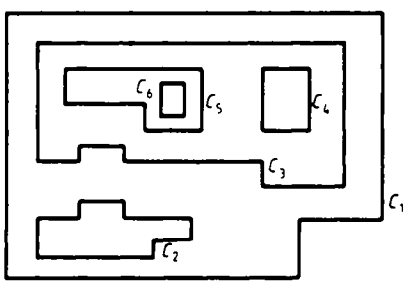

Figure 6. Hierarchical structure of frustrated contours.

3.5. Rigidity analysis

In some cases where $J_{ij} = \pm 1$ for instance there is no unique optimal solution of (P). Instead of using this degeneracy property of ground states, it is more relevant to use the concept of solidary spins to study the correlations between spins.

A packet of solidary spins is defined as a group of spins that keep the same relative orientation in all ground states. Such packets provide a measurement of the rigidity property and can be characterised by the set of *rigid bonds* (in contrast to *living bonds*).

A *rigid* bond is by definition an edge keeping its two spins in the same relative orientation in all ground states. Such a bond may be violated or not for all the ground states. A *living* bond is by definition a non-rigid bond (violated in some ground states, and non-violated in others).

When we compare two ground states it appears clearly that one (or more) packet of solidary spins is flipped as a whole. In this way the rigidity analysis yields information about the correlations between spins.

The naive way to study rigidity consists in a naive enumeration of ground states. Such a method becomes impracticable when the number of ground states is relatively high (in the frustration model, with $J_{ij} = \pm 1$, such a number becomes of the order of 10^{10} for samples of size 15×15).

Instead, the Chinese postman's algorithm permits a non-enumerative method giving a complete characterisation of the rigidity in a computation time proportional to a power law of the total number of spins.

Without loss of generality we briefly describe this method in the case $J_{ij} = \pm 1$. To find the set of rigid bonds, we use the following procedure. Starting with a ground state (solution X_0 of (P)), a violated bond is a living bond if and only if, for any $\varepsilon > 0$ added to its weight C_{ij}, we destroy the optimality of X_0. Otherwise this bond is a rigid bond (see figure 7).

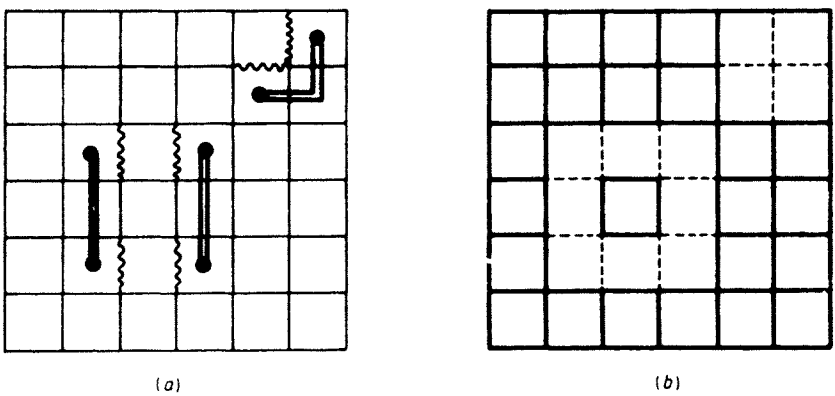

Figure 7. The wavy bonds indicate $J_{ij} = -1$, the straight bonds $J_{ij} = +1$. (*a*) One particular optimal solution. (*b*) Rigidity of the sample (*a*). The heavy bonds are rigid, the light bonds are living bonds.

This post-optimal analysis (it requires two new solutions for each bond, starting from X_0) can be done by a polynomial algorithm, as above. In fact, the algorithm of rigidity has $O(N_s^2)$ as complexity (Barahona 1980), where N_s denotes the total number of spins.

Details of this algorithm, as well as its complexity, are discussed in the following section.

NB The extension of the rigidity analysis, as well as its algorithmic description (ε rigidity) in the case $J_{ij} \in R$, cannot be discussed here, and will be published elsewhere.

3.6. Summary of the algorithm

To our knowledge the Chinese postman algorithm is the *first* one able to give in a non-ambiguous way the set of rigid bonds in the frustration problem. We shall give here a summary of this algorithm, keeping a detailed discussion for the Appendix.

Let $\overline{C_{ij}} = C_{ij} - \Sigma_{\{S|(ij)\in C=\delta(S)\}} y_s$ be the *reduced* weight of an edge (ij), where $C_{ij} = |J_{ij}|$. The 'complementary slackness' conditions can be stated as follows:

(i) $x_{ij} > 0 \Rightarrow \overline{C_{ij}} = 0$,

(ii) $y_s > 0 \Rightarrow \Sigma_{(ij)\in C=\delta(S)} x_{ij} = 1$.

A given configuration of spins can be viewed as a matching between frustrated plaquettes. The chains of this matching yield a feasible solution of (P): $x_{ij} = 1$ for edges belonging to this matching, and $x_{ij} = 0$ otherwise. Thus any configuration of spins gives a feasible solution X.

For simplicity, we give a simple procedure in two steps for the implementation of the algorithm.

(*a*) *Starting solution X.*

(1) To each chain joining two plaquettes u and v, we add an edge (u, v) to the matching, having the weight of the chain. For instance, if $J_{ij} = \pm 1$, this weight is nothing other than the length of the chain.

(2) A variable $y_{\{v\}}$ is associated with each frustrated plaquette; this variable is equal to the chain weight, having v as extremity.

All other contours S are absent, $y_s = 0$.

Thus we have a pair (X, Y), satisfying (i) and (ii) and X is a feasible solution of (P).

(*b*) *Solution Y:* In this second step, (X, Y) are changed:

(1) so that X remains feasible;

(2) to minimise $\Sigma_{(ij)} |J_{ij}| x_{ij}$ and to bring Y feasible;

(3) to maintain (i), (ii) satisfied.

The algorithim alternatively leads to a pair of optimal solutions (X, Y).

4. Numerical experimentation

The numerical simulation is performed on a square lattice of Ising spins σ_i. The bonds between spins J_{ij} are chosen as independent random variables from the probability law

$$P(J_{ij}) = x\delta(J_{ij} + J) + (1 - x)\delta(J_{ij} - J).$$

This is the well known random $\pm J$ model of spin glasses.

The purpose of the numerical simulation is to study the evolution of the structure of the ground states when the concentration x of negative bonds is increased.

The samples are constructed first by assigning a specific random number to each bond, then assigning the k smallest values of the set of random numbers as negative bonds. By increasing the value of k, a family of samples is generated by adjunction of negative bonds $-J$ to the previous sample. For each member of the family, a particular ground state is obtained as well as the map of rigid bonds for all ground states. Three different sizes are studied (10×10, 15×15, 20×20) with different concentrations of frustrated plaquettes; all the samples are characterised in table 1. The average concentration of frustrated plaquettes for an infinite sample is given by

$$C_p(x) = 4[x(1 - x)^3 + x^3(1 - x)]$$

but for a finite sample, fluctuations around this mean value arise. Since the number of frustrated plaquettes must be fixed, the concentration of negative bonds is varied until the expected number is reached. Around $C_p = 0.5$, x is chosen to be closest to 0.5. But it turns out that the best variable for building classes of samples is the number of unsatisfied bonds or even the energy (cf § 5) rather than C_p or x.

The boundary conditions play a very important role in the analysis of results and will be detailed here. We have introduced joining edges in the vertical and horizontal rows

of the spin lattice which produce the standard toroidal mapping for a planar lattice. In the dual lattice of plaquettes, on the contrary, the two new cycles ('superplaquettes') which cannot be obtained by symmetrical difference of elementary frustrated plaquettes (Bieche *et al* 1980) are ignored and the graph remains planar. These conditions are not the standard periodic conditions and will be called 'pseudo-periodic conditions'. Another type of boundary condition used in an equivalent way is the pseudo-antiperiodic condition. In this case the joining edges for the toroidal mapping couple the spins of the last line or row (i or $j = L$) with the spins of an additional line or row (i or $j = L + 1$) obtained from those of the first line (i or $j = 1$) by reversing their orientation. This is an additional degree of freedom for the algorithm which takes the possibility of optimising the ground-state energy by changing the boundary conditions from pseudo-periodic to pseudo-antiperiodic or *vice versa*.

The correct picture of these boundary conditions is the repeated cell scheme or the tesselation of the plane. For the pseudo-antiperiodic conditions the primitive cell is a larger square, the length of which is twice the length of the initial sample. These boundary conditions permit us to exhibit the magnetic wall structure for moderate values of x.

5. Results

For each sample of the set of 248 samples described in table 1 a ground state has been represented as well as the map of the rigid bonds. From the analysis of these maps, three main points emerge:

(1) decrease of rigidity and fracturation,
(2) non-standard percolation of rigid bonds,
(3) random antiphase state and magnetic walls at moderate concentration.

5.1 Rigidity and fracture lines

Three typical situations are reported in figure 8: *rigid sample* (8(a)) where the cluster of rigid bonds reaches the four sides (percolating cluster) at low concentration of negative bonds or frustrated plaquettes; once vertically *fractured sample* (8(b)) where the cluster

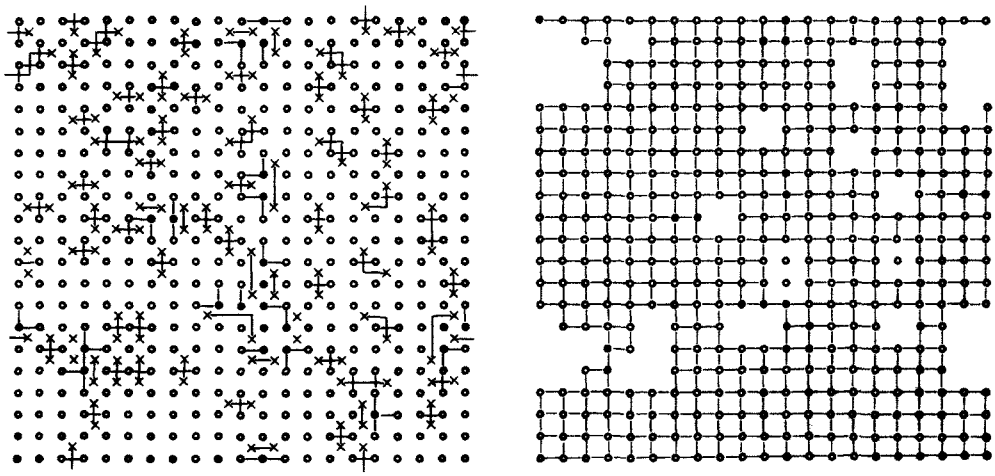

(a)

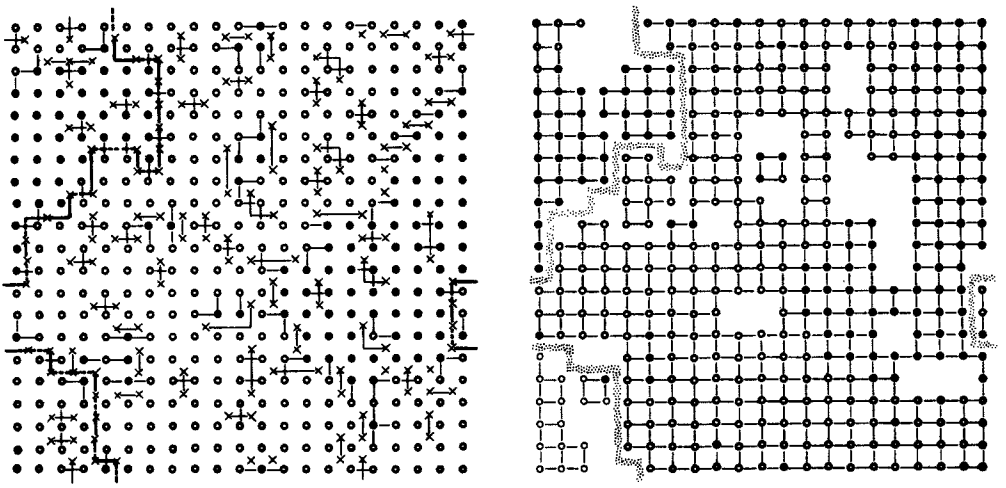

(*b*)

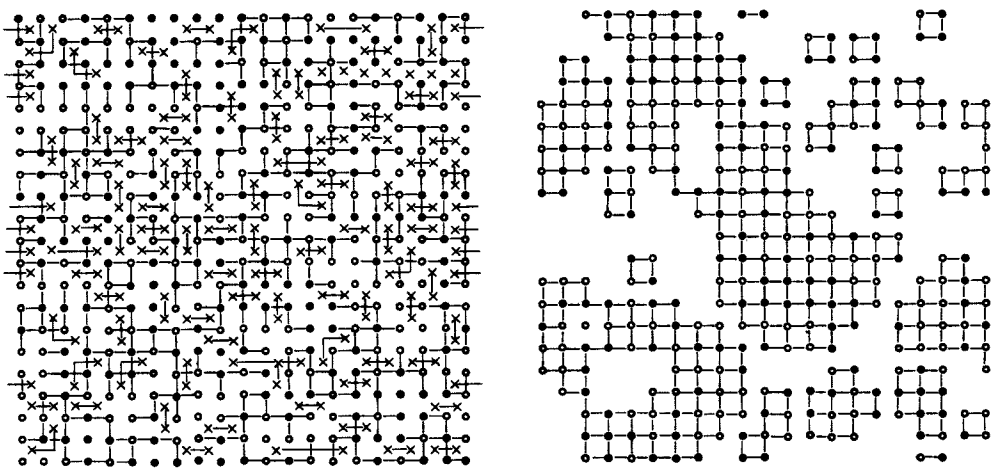

(*c*)

Figure 8. *Fracturation by frustration.* The samples exhibited in (*a*), (*b*) and (*c*) contain 20×20 Ising spins, the orientations of which are up for the open circles and down for the full circles. The periodic conditions are used and the 21st line or row repeats the first one. On the left of each figure one particular ground state is shown; the right hand parts exhibit the map of rigid bonds (straight segments) while the living bonds are omitted. On the left part, the strings joining the spins represent negative bonds. The frustrated plaquettes are represented by crosses in the centre of the plaquettes. The strings joining the plaquettes indicate the violated bonds. The three samples belong to the same family. They are generated by adding negative bonds to the initial sample. All these ground states have periodic boundary conditions. (*a*) *Ferromagnetic ground states.* The concentration of negative bonds is $x = 0.12$. The rigid bonds constitute a large percolating cluster. The holes in the lattice indicate living bonds and loose spins. (*b*) *Fracture line* ($x = 0.146$). The cluster of rigid bonds does not percolate in the horizontal direction. In the corridor delimited by the rigid bonds a fracture line runs from the upper side to the bottom. On the left-hand side of the figure, the fracture line is built up from alternating strings—straight and broken—in equal number, in such a way that the spins in the right part of the sample can be reversed without any cost in energy. Therefore there are equal numbers of straight and broken bonds. (*c*) *Complete fracturation* ($x = 0.5$). The clusters of rigid bonds are of finite size. There are many fracture lines in the corridors between the clusters but they are not shown. Each cluster reveals strong fluctuations of magnetisation like ferromagnetic grains. No long-range magnetic correlation can survive in this situation.

of rigid bonds does not percolate in the horizontal direction; completely fractured sample represented in figure 8(*c*), where the cluster becomes of small size and does not percolate in any direction.

The examples exhibited in figure 8 have been chosen on the basis of representativity of average trends: a fracturation of samples into small clusters appears when the concentration of negative bonds x or frustrated plaquettes C_p increases.

This fragmentation of an 'infinite' cluster into 'finite' clusters can be analysed quantitatively in terms of the fraction of rigid bonds in the largest cluster of rigid bonds F, as for the standard percolation problem. However it turns out that the variables x or C_p lead to a large spreading out of the data, while the energy variable E_0 or equivalently the number of unsatisfied bonds N_{ub} gives better plots. The correspondence between E and N_{ub} is $E/N_sJ = E_0 = -2(1-\phi)$ where $\phi = N_{ub}/N_s$ and we use the monotonic curve $E_0(x)$ of figure 8 from Bieche *et al* (1980) to determine the corresponding x values. The function $F(\phi)$ is plotted in figure 9; each value is the fraction of rigid bonds in the largest cluster averaged over a class of samples characterised by a given N_{ub} and size. The points show undoubtedly a decrease of $F(\phi)$ expressing the progressive fracturation of the samples. We expected a steeper decrease for larger size (a step function for infinite size at the critical threshold), but this is not observed because of the too small number of samples of sizes 15×15 and 20×20, respectively 56 and 32. By analogy with the numerical study of percolation (Roussenq *et al* 1976), we locate the threshold at $F = 0.5$, giving $N_{ub} \simeq 0.26$ and, from figure 10, $x_c \simeq 0.15$. This numerical determination of x_c confirms the previous published value (Bieche *et al* 1980).

But the principal interest of this result is the disappearance of any long-range order above x_c, particularly at $x = 0.5$. As a matter of fact any correlation of staggered magnetisation ranging to infinity implies infinite rigid clusters; the fracturation of infinite clusters demonstrates therefore the finite range of the correlation above x_c. This study confirms the conclusions of Morgenstern and Binder (1980) at $T \simeq 0$ K in two dimensions, but disagrees with the previous numerical study of Vannimenus *et al* (1979) who found a bigger rigidity at $x = 0.5$. The discrepancy probably originates in their use of the Monte Carlo method of relaxation, which does not permit an exact average over all the ground states or even the low-energy excited states.

An alternative but equivalent way to describe this transition of fragmentation into small clusters is the occurrence of fracture lines in the samples. Such a fracture line has been defined in great detail by Bieche *et al* (1980): it corresponds to an alternating cycle of equal numbers of satisfied and unsatisfied bonds in such a way that the permutation of the set of bonds is possible at constant energy.

Moreover, this line must cross the sample from one side to the opposite one. In other words, these lines cannot run in the rigid bonds of the clusters and generally surround them in the region of living bonds. Figure 8(*b*) exhibits this kind of line which runs in the corridor between the clusters of rigid bonds. We have systematically looked for the existence of these lines in the set of samples and constructed the frequency of occurrence as a function of the energy variable. (The presence of this fracture line excludes the percolating cluster of rigid bonds and *vice versa*). This probability is plotted in figure 10 and shows an abrupt increase around the value $N_{ub} \simeq 0.25$ corresponding to $x_c \simeq 0.15 \pm 0.01$. This value coincides as expected with the threshold of fragmentation observed in figure 9.

Therefore the previous description of the fragmentation of the clusters of rigid bonds can also be obtained by inspection of the occurrence of fracture lines: its proliferation above $x_c \simeq 0.15$ coincides with the pulverisation in small and finite clusters.

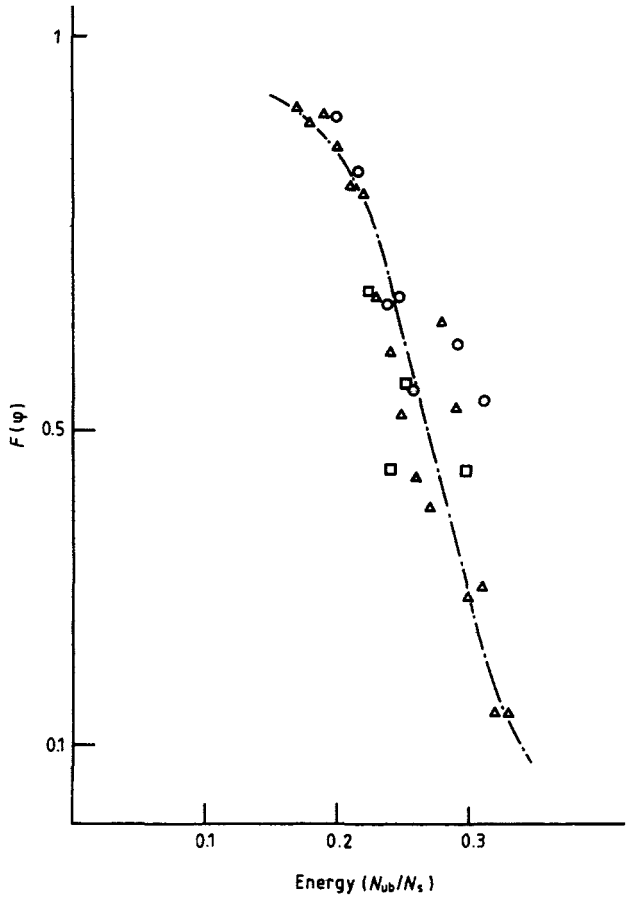

Figure 9. For each size, the samples are regrouped into classes of ground-state energies in units of the number of unsatisfied bonds over the number of spins. There is a one-to-one correspondence between these values and the concentration of negative bonds in figure 7 of Bieche *et al* (1980). For instance, the value $N_{ub}/N_s = 0.2$ corresponds to $x = 0.1$ while $N_{ub}/N_s = 0.3$ corresponds to $x = 0.19$. The strong decrease of the fraction of rigid bonds in the largest cluster by increasing N_{ub}/N_s or x points out the fracturation of the large cluster of rigid bonds at low x (figure 8(a)) into small finite clusters for $x \simeq 0.5$ (figure 8(c)). There is large scattering of the data which prevents an analysis of the disappearing of rigidity in terms of finite-size scaling. The chain curve is an averaging curve among the points. △, 10×10 (155 samples); ○, 15×15 (156 samples); □, 20×20 (32 samples).

5.2. Percolation of rigid bonds

A glance at figure 8 reveals for an expert eye a strong geometrical difference between the percolating cluster of rigid bonds and the standard percolation of bonds in the square lattice. In particular, the compactness of the clusters is stronger here: there is an absence of dangling bonds since a given spin cannot stay rigid when it is surrounded by three loose spins.

In view of pointing out this distinction, the probability of percolation (or frequency of percolating clusters in a given class) has been calculated for the subset of percolating clusters (figure 8(a)) as a function of the concentration of rigid bonds. The curve is represented in figure 11 and exhibits a threshold of percolation at $C_R \simeq 0.7$. (For an infinite sample the curve should be a step function.)

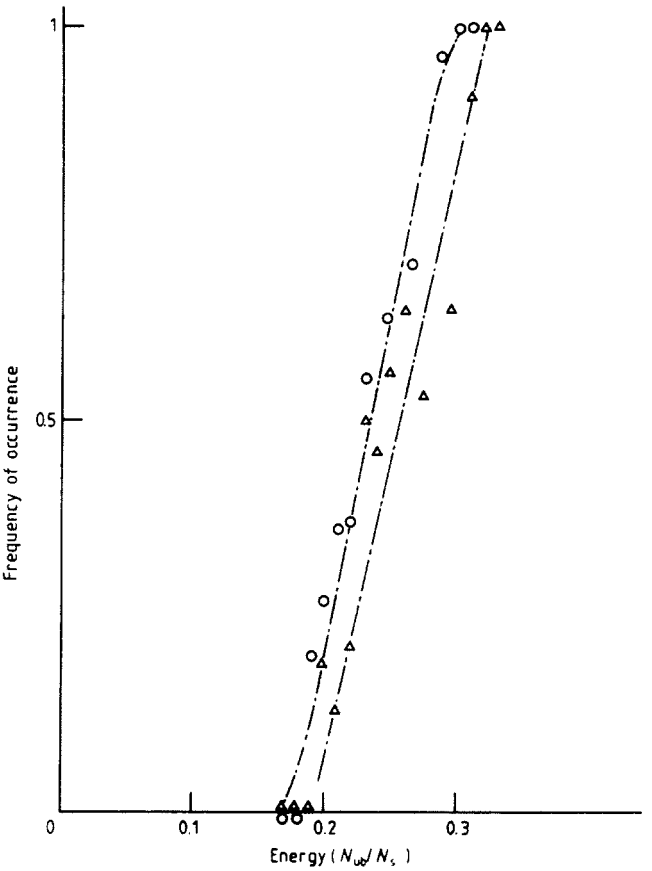

Figure 10. The total number of samples of sizes 10×10, 15×15 and 20×20 are regrouped into classes of ground-state energies in units of N_{ub}/N_s. The frequency of occurrence of (at least) one fracture line for each class is represented by triangles (243 samples). The occurrence of magnetic walls is looked for only in the rigid samples (number 173). The frequency of occurrence for the magnetic walls is represented by circles. The chain curves are average curves among the data. The thresholds defined by the value of N_{ub}/N_s corresponding to 0.5 are identified as $x_m = 0.10$ and $x_c = 0.15$.

This value is larger than the known threshold for the uncorrelated model of bond percolation on the square lattice, $C_p = 0.5$. This difference is a direct consequence of the strong correlation of rigid bonds resulting from the presence of interacting spins at the origin of the rigidity.

5.3. Random antiphase state and magnetic walls

The rigid samples (samples with an 'infinite' cluster of rigid bonds) occur at low concentration $0 < x \leqslant 0.15$, where the ferromagnetic ground state is expected. Actually a finer analysis of the samples shows a more subtle situation regarding the boundary conditions. We observe that the set of rigid samples ($x \leqslant 0.15$) can be divided into two classes:

(1) a low-concentration class $x \leqslant 0.10$ where the pseudo-periodic conditions are almost always chosen by the algorithm (ferromagnetic ground state);

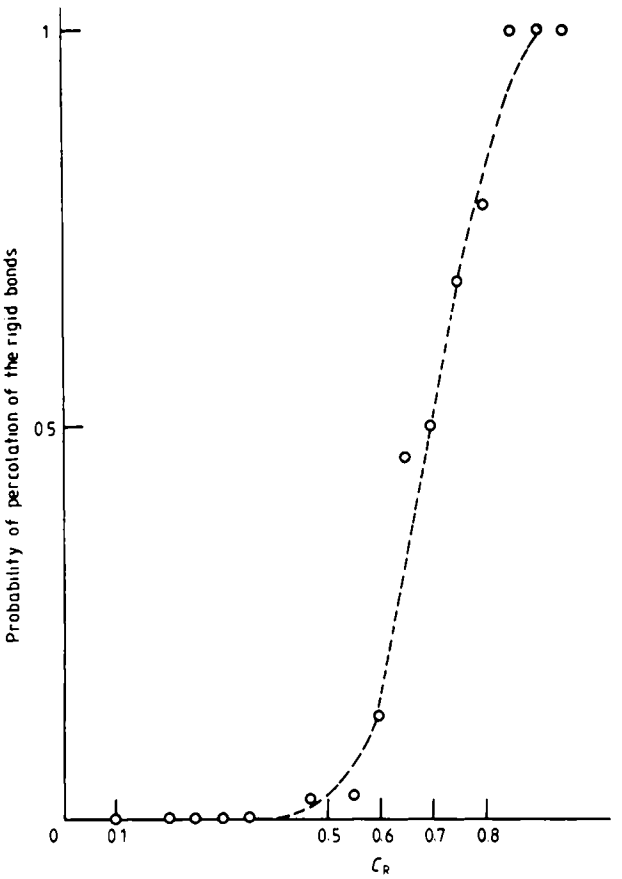

Figure 11. Probability of occurrence of a percolating cluster of rigid bonds as a function of the concentration of rigid bonds.

(2) a moderate concentration class $0.10 \leqslant x \leqslant 0.15$ where the pseudo-antiperiodic conditions are found more often.

This observation is illustrated by the samples of figure 12, where the boundary condition passes from the periodic to the antiperiodic case when the concentration increases from the low-concentration regime into the moderate-concentration regime. For this situation there are two important implications from this antiperiodicity, occurrence of (at least) one magnetic wall, and zero magnetisation. In figure 12(*b*) a magnetic wall is drawn which runs through the sample. This line separates the domain of spins up from that of spins down, but is 'macroscopic' as a domain wall in the sense that it crosses the sample from one side to the opposite side. The same wall is drawn on the left side of figure 12(*b*) and its path runs partly on the loose bonds and partly on the rigid bonds of the 'infinite' cluster. The path of this line is unique in the infinite cluster because of rigidity but not unique in the domain of living bonds. Since the loose spins have no well defined directions, the path of this line is diffuse in this region of the sample. It is not so easy to realise the 'macroscopic' character of the magnetic wall from figure 12(*b*): a better visualisation of this situation appears in figure 13 where the repeated cell scheme is drawn. The antiperiodicity along the vertical axis imposes a double cell as primitive zone, and the representation of antiphase magnetic domains

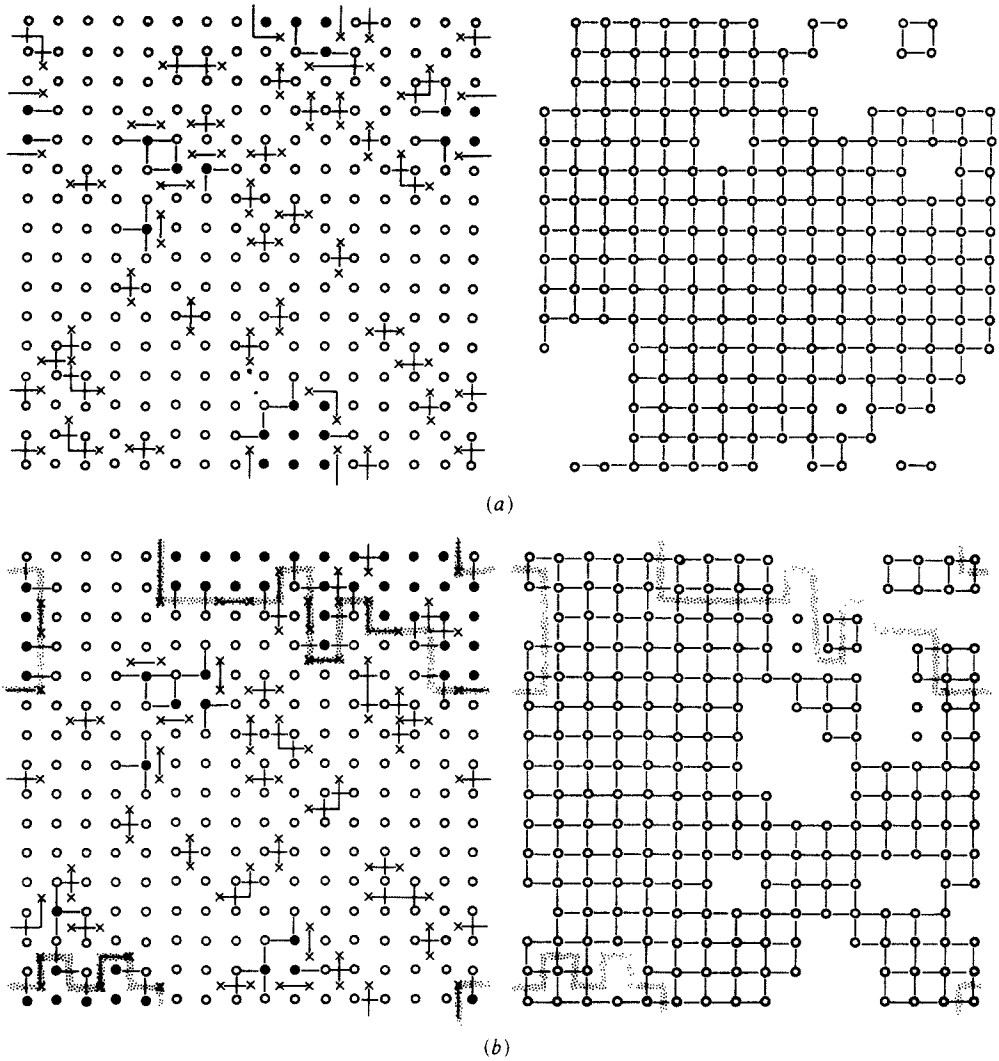

Figure 12. *Magnetic wall.* As figure 8 except the size of the samples: 15×15. (*a*) *Ferromagnetic ground state* ($x = 0.135$). The periodic boundary conditions are used on vertical and horizontal sides. (*b*) *Random antiphase state* ($x = 0.17$). The antiperiodic boundary conditions are used on the horizontal sides while the periodic ones exist on vertical sides. A magnetic wall is represented by dotted lines. It separates the spins in two domains: up and down orientations correspond to white and black circles. Here the magnetic wall runs across the percolating rigid cluster as well as the living bonds. The left-hand figure corresponds to one particular ground state: it is shown that this defect line is composed of satisfied negative bonds and unsatisfied positive bonds in unequal proportions.

and the path of magnetic walls shows the structure of the ground states in the antiphase state. It is obvious that the magnetisation vanishes in this case since any strip of given orientation has its own replica with reversed magnetisation. (Among the 173 samples analysed in this way we have also observed two cases where, despite the periodicity of the boundaries, two magnetic walls ere present simultaneously. There, the magnetisation was not strictly zero but very small.) In order to delimit this new phase (random

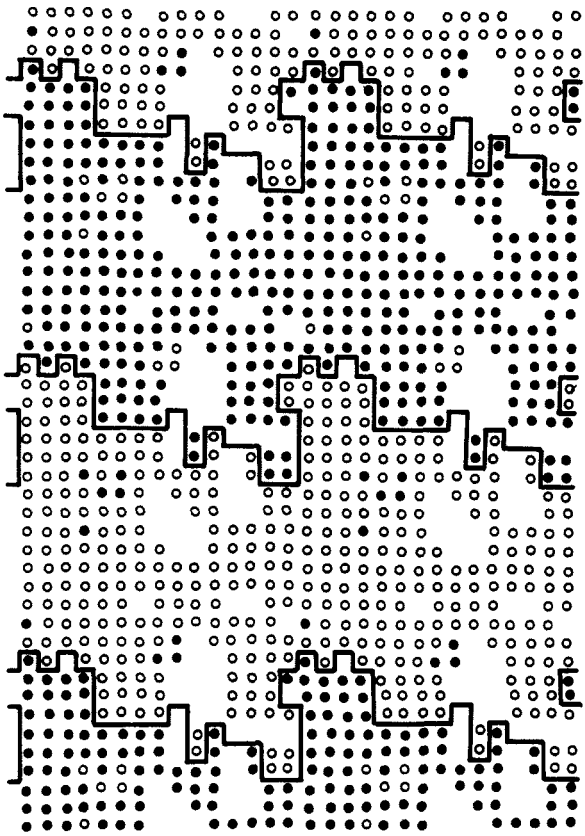

Figure 13. *Random antiphase state.* This figure is a repeated zone scheme of figure 12(*b*) which exhibits the macroscopic nature of the magnetic wall separating the domains of opposite spins. The magnetisation is, therefore, equal to zero. For the detailed legend, see figure 8.

antiphase state) we have looked for the presence of magnetic walls in the set of *rigid* samples, i.e. samples possessing an 'infinite' cluster of rigid bonds. In figure 10 the points represent the frequency of occurrence of these defects among 173 samples. Since this curve must become a step function in the limit of an infinite sample, the threshold is taken at the value 0.5 for the frequency which corresponds to a fraction $\phi = 0.23$. By using the relation between energy and this fraction $E/N_s J = E_0 = -2(1 - N_{ub}/N_s)$, the ground-state energy is $E_0 = -1.54$, which gives $x_m = 0.1$. Although the determination of this value is imprecise, its value is by construction less than $x_f \simeq 0.15$: $x_m < x_f$, because the random antiphase state is defined only for the rigid samples.

6. Discussion and conclusions

This study has two objectives: to generate exact ground states of the frustration model by an elaborate algorithm which overcomes the difficulties of the standard Monte Carlo method, and to analyse the structure of all the ground states. The first objective is

reached by the correspondence set up between this problem and that of the Chinese postman. The algorithm of Edmonds gives the possibility to find the minimum of the energy by constructing a dual problem where the minimum is reached by optimising successively the primal and then the dual problem. The concept of frustration or frustrated cycle turns out to be the most relevant variable for this problem: the relaxation towards the minimum can be described as a flip of packets of solidary spins of any size or shape. This algorithm is polynomial and varies as $O(N_s^3)$ even for determining the map of rigid bonds, a property characteristic of all the ground states.

The analysis of the samples leads to the existence of two types of defects: fracture lines and magnetic walls. If the first category has been already conjectured (Vannimenus and Toulouse 1977, Bray *et al* 1977, 1978, Bieche *et al* 1980), the second one is revealed by this study. It is important to notice the distinction between these two lines defects.

The fracture lines are the alternating cycles of an equal number of satisfied and unsatisfied bonds in such a way that the energy is invariant under a change of the matching. Nothing refers to the nature of these bonds—positive or negative J_{ij}—nor to the orientations of the spins—up or down. The fracture line creeps along the corridor between the clusters of rigid bonds. It indicates a destruction of the macroscopic rigidity and implies that the magnetic correlation between spins belonging to two different clusters vanishes. From the observed occurrence of these fractures above $x_c \simeq 0.15$ we conclude that no long-range correlation can persist above $x_c \simeq 0.15$. Actually there is no long-range order of any type: the concentrated regime is a purely disordered phase or superparamagnetic phase ('super' because it subsists here a finite range for rigidity leading to clustering of spins).

The magnetic wall appears in a quite different context: it is found when the samples are rigid, below $x_c = 0.15$, and it is constituted by an *unequal* number of *satisfied negative bonds* and *unsatisfied positive bonds*. There is no balance between satisfied and unsatisfied bonds: an alternation or pivot of the matching gives an increase of the energy. The energy of this defect is therefore negative in the range of the antiphase state while the energy of fracture lines vanishes above $x_c = 0.15$. Since this random antiphase state exists in the range of rigidity the magnetic correlation of the spins (in the rigid cluster) is equal to one. This extreme correlated state, however, must be analysed by local reference systems into each antiphase domain: it corresponds to a random staggered magnetic correlation in analogy with the case of the Mattis model. Then the random antiphase state is a genuine ordered state at $T = 0$ K for which the staggered correlation function is equal to 1.

In summary, the morphology of ground states evolves in the following way: at very low concentration of negative bonds the ground states are ferromagnetic with a very small density of loose spins and a still smaller concentration of down spins. By increasing the concentration, a state is reached where the loose spins are still small and confined, while magnetic walls appear and break the ground states into antiphase domains. This is the random antiphase state appearing between $0.10 \leqslant x \leqslant 0.15$. Above x_c the domain of loose spins percolate and the fracture lines proliferate: the finite packets of solidary spins are also structured in antiphase domains, while around $x \simeq 0.5$ these finite packets become very small and look like antiferromagnetic grains. Therefore, at $T = 0$ K, three distinct phases are encountered along the x axis: $0 < x \leqslant 0.10$ a ferromagnetic phase, $0.10 \leqslant x \leqslant 0.15$ the random antiphase state and $x \geqslant 0.15$ the superparamagnetic phase.

All these results are obtained for the $\pm J$ model at $T = 0$ K. The possible generalisation of these results to a continuous distribution $P(J)$ like the gaussian model needs a

new definition of the rigidity. In a $\pm J$ model the rigidity of bonds is a property common to all the ground states. In a continuous $P(J)$ model there is only one ground state but a large density of low-energy excited states. In this case, a natural generalisation of the rigidity is the ε rigidity, where the stability of one perfect matching is tested by changing the bond interaction J by a finite quantity ε. Indeed, for $\varepsilon \to 0$ all the bonds are rigid but this number decreases by increasing ε. An interesting question would be to estimate ε which would give approximatively the same clustering of spins as the $x = 0.5$ case. To answer this question we can use the comparative numerical study of these models by Morgenstern and Binder (1980).

From an exact solution of the finite-size sample, they obtained numerically the entropy function for both the $\pm J$ and gaussian $P(J)$ models as a function of temperature. The residual entropy at $T = 0$ K is finite for the $\pm J$ model: $S/k_B \simeq 0.075$.

The temperature T_0 for which $S(T_0) = 0.075$ in the gaussian $P(J)$ model is approximately $T_0 \simeq 0.3$. This value could give an estimate $\varepsilon \simeq 0.3$ for which the analyses of ground-state structures are similar in both models. In the same way, the average interaction $1-2x$ would correspond to the first moment of a shifted gaussian distribution $P(J)$. We believe that most of these results for ground states of the $\pm J$ model are transposable for the low-energy or low-temperature states of the continuous $P(J)$ model. Thus the property of fragmentation into finite rigid clusters is likely to be a $T \simeq 0$ K property of the continuous $P(J)$ model. In the same way, the random antiphase state discovered for the $\pm J$ model might be stable when $P(J)$ becomes continuous.

Acknowledgments

It is a pleasure for the authors to acknowledge stimulating discussions and correspondence with Professor G Toulouse and Dr J Vanimenus.

Appendix 1. A primal algorithm for the Chinese postman's problem

A1.1. Strategy

The Chinese postman's problem has been solved by Edmonds and Johnson (1973), using matching theory. They gave a description of the polyhedron of solutions using a dual algorithm. The inconvenience of using a dual algorithm is that only at the final step have we a solution that corresponds to a spin configuration. We have made a slight modification of their algorithm to obtain a primal algorithm.

In this way, any transient solution corresponds to a spin configuration, and each step consists in reversing a spin cluster in order to decrease the total energy.

To be more precise, for a given graph $G = (V, E)$ a set of 'odd nodes' $\sigma \subseteq V$, with even cardinality and edges weights $w_e \geqslant 0$, $e \in E$, we will solve the following problem.

(1) Minimise $\Sigma_{e \in E} w_e x_e$ subject to

$$\sum_{e \in \delta(i)} x_e \equiv 1 \pmod 2 \text{ if } i \in O,$$

$$\sum_{e \in \delta(i)} x_e \equiv 0 \pmod 2 \text{ if } i \in V - O,$$

$$x_e \in \{0, 1\} \text{ for } e \in E.$$

For $S \subseteq V$, $\delta(S)$ denotes the set of edges having exactly one end in S, and for $v \in V$, we abbreviate $\delta(\{v\})$ as $\delta(v)$. We set $Q = \{S \subseteq V \mid |S \cap \sigma| \text{ is odd}\}$, the family of 'odd sets' ($|A|$ denotes here the cardinality of set A).

Following Edmonds and Johnson, (1) is equivalent to

(2) minimise $Z = \Sigma_{e \in E} w_e x_e$ subject to

$$\sum_{e \in \delta(S)} x_e \geqslant 1, \qquad S \in Q, \qquad x_e \geqslant 0, \qquad e \in E.$$

The dual of this linear program is

(3) maximise $v = \Sigma_{S \in Q} y_s$ subject to

$$\sum_{\{S \in Q \mid e \in \delta(S)\}} y_s \leqslant w_e, \qquad e \in E,$$

(4) $$y_s \geqslant 0, \qquad S \in Q.$$

If X is a feasible solution of (2), and Y a feasible one of (3), X and Y are optimal solutions if and only if the following 'complementary slackness' conditions are satisfied (Dantzig 1962):

(5) if $x_e \geqslant 0$ then $\Sigma_{\{S \mid e \in \delta(S)\}} y_s = w_e$,

(6) if $y_s > 0$ then $\Sigma_{e \in \delta(S)} x_e = 1$.

The algorithm we will describe maintains a feasible solution X of (2) with Y satisfying (4), (5), (6), but initially it does not require the feasibility of (3). The algorithm will modify X and Y, until Y becomes feasible.

A1.2. Shrinking operation

We define the operation of shrinking $S \in Q$ as replacing all nodes in S by a pseudonode P with $\delta(P) = \delta(S)$. In fact, we connect all nodes adjacent to a node in S to the pseudonode P (see figure 14).

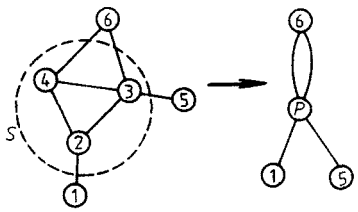

Figure 14. Shrinking operation.

Unshrinking S is the inverse operation. At any step of the algorithm, we will have a surface graph G_S obtained by shrinking some odd sets in G.

The initial solution will be a pair (X, Y) where X is the characteristic vector of a set of simple chains joining the nodes of O, with Y satisfying (4), (5), (6), and where $F = \{S \in Q \mid Y_s > 0\}$ is a nested family. The initial graph G_S is obtained from G by shrinking all sets in F.

We let $\bar{w}_e = w_e - \Sigma_{\{S \mid e \in \delta(S)\}} y_s$ be the reduced weight of edge e.

A1.3. Algorithm

Step 1. If $\bar{w}_e \geq 0$ for any $e \in E$, stop. Otherwise, let $a = (k, 1)$ be an edge such that $\bar{w}_e < 0$.

Step 2. Give the label '$-$' to the outer odd set S such that $y_s > 0$ and one extremity of a belongs to S. Let k be this extremity.

Apply the labelling subroutine.

Step 3. If the other extremity l is labelled '$+$', perform a primal change (step 5).

Otherwise, perform a dual change (step 4).

Step 4. Set $\varepsilon_1 = \min\{\bar{w}_e \mid e = (ij),\ i$ is labelled '$+$', j is not labelled and $\bar{w}_e \geq 0\}$.
$\varepsilon_2 = \min\{\bar{w}_e/2 \mid e = (ij),\ i$ and j are in different pseudonodes labelled '$+$' and $\bar{w}_e \geq 0\}$.
$\varepsilon_3 = \min\{y_s \mid S$ is labelled '$-$'$\}$.
We define $\min\{h : h \in \varnothing\} = +\infty$. Set $\omega = \min\{\varepsilon_1, \varepsilon_2, \varepsilon_3\}$, and change Y as follows:

$$y_s \leftarrow \begin{cases} Y_s - \omega \text{ if } S \text{ is labelled '}-\text{'} \\ Y_s + \omega \text{ if } S \text{ is labelled '}+\text{'} \end{cases}$$

If $\delta = \varepsilon_3$, unshrink pseudonodes P labelled '$-$', so that $y_p = 0$.

Go to step 2.

Step 5. There is a path of edges with reduced weight equal zero, form k to l, that permits a primal change. Perform

$$x_a \leftarrow 1,$$
$$x_e \leftarrow 1 - x_e \text{ for each edge } e \text{ in the path.}$$

In order that $\bar{w}_a$ becomes zero, execute the following procedure. While $\bar{w}_a < 0$, do:

let P be a pseudonode such that $a \in \delta(P)$;
set $\delta = \min\{y_p, -\bar{w}_a\}$;
perform $y_p \leftarrow y_p - \delta$;
if $y_p = 0$ unshrink the pseudonode P.

A1.4. Labelling subroutine

L1. If the pseudonode i has the label '$-$', make a list of all the nodes and pseudonodes connected to i with edges e such that $x_e = 1$. Make with this list an odd set, shrink it and label it '$+$'. (Figure 15(a)).

L2. If the pseudonode i is labelled '$+$', scan edges in $\bar{\delta}(i) = \{e = (ij) \in \delta(I) \mid x_e = 0, \bar{w}_e = 0\}$.

(i) If j is labelled '$+$', make a blossom (L3).

(ii) If j is an unlabelled pseudonode, label it '$-$', apply (L1) to j and continue to scan edges in $\bar{\delta}(I)$.

(iii) Otherwise, make a list of all nodes and pseudonodes connected to j with edges e such that $x_e = 1$; enter i in this list; delete the label of i; make an odd set with this list; shrink it and label it '$+$' (see figure 15(b)).

L3. There are two different paths from k to label the pseudonode j (see figure 15(c)). Let $k, v_1, \ldots, v_r, n_1, \ldots, n_p, j$ and $k, v_1, \ldots, v_r, m_1, \ldots, m_q, j$ be the two paths. Make

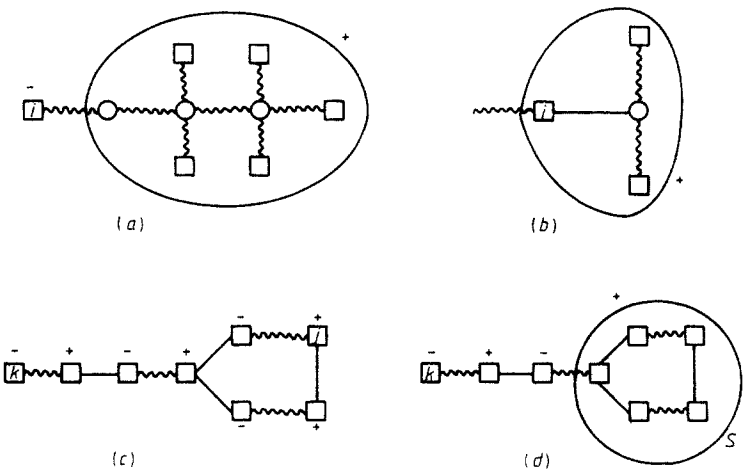

Figure 15. Labelling operations.

$S = \{n_1, n_2, \ldots, n_p, m_1, \ldots, m_q, v_r, j\}$ an odd set. Delete the labels of elements of S, shrink it, and label it '+'. (See figure 15(d)).

A1.5. The initial solution

Let $\sigma = \{v_1, \ldots, v_{2k}\}$, the set of odd nodes. An initialisation can be obtained by finding a path between v_{2p-1} and v_{2p} for $p = 1, \ldots, k$. Let l_p be the total weight of this path. Add an artificial edge between v_{2p-1} and v_{2p} with weight l_p, for $p = 1, \ldots, k$. Set to 1 the variable x associated to artificial edges and to zero the other variables x. Construct the odd sets $\{v_1\}, \{v_2\}, \ldots, \{v_{2k-1}\}$, with dual variables equal to $l_1, \ldots, l_p(m)$ respectively and shrink them. This initialisation represents the spin configuration obtained by frustrating bonds in the path between v_{2p-1}, and v_{2p} for $p = 1, \ldots, k$.

A1.6. Discussion of the algorithm

This algorithm gives the solution of the frustration problem for any given weight J_{ij} of edges in the planar graph G. Each step of the algorithm that modifies X or Y preserves the properties required to the initial solution. The dual changes are such that the reduced weights that are not negative do not become negative. For each negative reduced weight, at most $O(|v|)$ applications of the labelling subroutine are required. Fr a planar graph, a bound to the amount of work of a labelling is an $O(|v|)$ calculation, and there are at most $O(|v|)$ negative reduced weights. Then a bound to the amount of work of the algorithm is an $O(|v|^3)$ elementary calculation. For instance, in a square lattice, where $V \simeq L \times L$, the amount of work is $O(L^6)$. Thus, we have a polynomial algorithm for the frustration problem on planar graphs. The situation changes in a dramatic way if we relax this property. In fact, we can show (Barahona 1980) that the problem of frustration becomes *NP*-complete on 3D lattices. This 'crossover' occurs for $L \times L \times 2$ lattices! It is not clear to the authors if this change of algorithmic complexity will have a physical signification.

A1.7. The rigidity

We will describe a straightforward procedure to determine rigid bonds. We suppose that edge weights have integers greater than or equal to 1 ($|J_{ij}| \geq 1$).

After finishing the algorithm, we can label as rigid, edges with reduced weight strictly positive. Because of condition (4), their variable x will be zero in all the optimal solutions. For an edge e with $x_e = 0$ and $\bar{w}_e = 0$ we subtract $\varepsilon = \frac{1}{2}$ from w_e and we apply the algorithm. If no primal change is necessary, the edge is rigid. If a primal change is necessary, we label as living bonds all edges interfering in the primal change. For an edge e with $x_e = 0$, we add y_2 to w_e, and we add $\frac{1}{2}$ to an odd set S, with $y_s > 0$, and such that $e \in \delta(S)$, in order to verify (4).

We apply the algorithm and the same analysis as above. The bound $O(|v|^3)$ to the amount of work of this procedure applies as for the algorithm above.

In the case where the edge weights are not integers, but real numbers, we must change the notion of rigidity. In fact, in such a case we have a band of low-energy excitation states. The notion of strict rigidity (see above) is to be replaced by that of ε rigidity, where $\varepsilon > 0$ is a given real number. This concept will be discussed elsewhere.

To end this Appendix it is interesting to make some remarks about this algorithm.

(a) First, the complexity of this algorithm is polynomial: $O(|v|^3)$.

(b) The computational procedure maintains primal and dual aspects at all times. In this sense this algorithm can be called primal–dual.

(c) To our knowledge this is the only polynomial algorithm able to give the rigidity of the ground state in the frustration problem on a planar graph.

(d) In contrast to the dual–primal algorithm, using the matching procedure directly (Bieche *et al* 1980), the primal–dual algorithm starts with a given configuration of spins, and progresses by improving this solution. At first sight this procedure seems to be analogous in spirit to the relaxation techniques. However, in contrast to standard relaxation procedures, successive steps correspond here to flipping spin clusters of any shape, and any size.

This is precisely the main reason for the failure (Rammal *et al* 1979) of the Monte Carlo method which is unable to execute such transitions.

References

Barahona F 1980 *These docteur ingenieur* Grenoble
Bieche I, Maynard R, Rammal R and Uhry J P 1980 *J. Phys. A: Math. Gen.* **13** 2553
Binder K 1980 in *Fundamental Problems in Statistical Mechanics* (Amsterdam: North-Holland)
Bray A J and Moore M A 1977 *J. Phys. F: Met. Phys.* **7** L333
Bray A J, Moore M A and Reed P 1978 *J. Phys. C: Solid State Phys.* **11** 1187
Dantzig G B 1962 *Linear Programming and Extensions* (Princeton, NJ: Princeton University Press)
Edmonds J 1965 *Operations Research* **13** Suppl **1** 373
Edmonds J and Johnson E L 1973 *Math. Programming* **5** 88
Kirkpatrick S 1977 *Phys. Rev.* B **16** 4630
Mei-Ko Kwan 1962 *Chinese Math.* **1** 273
Morgenstern I and Binder K 1980 *Phys. Rev.* B **22** 288
Orlova G I and Dorfman Y G 1972 *Engrg. Cybernetics* **10** 502
Parisi G 1979 *Phys. Rev. Lett.* **43** 1754
Rammal R, Suchail R and Maynard R 1979 *Solid State Commun.* **32** 487
Roussenq J, Clerc J, Giraud G, Guyon E and Ottavi H 1976 *J. Physique Lett.* **37** L99
Toulouse G 1977 *Commun. Phys.* **2** 115
Vannimenus J, Maillard J M and de Sèze L 1979 *J. Phys. C: Solid State Phys.* **12** 4523
Vannimenus J and Toulouse G 1977 *J. Phys. C: Solid State Phys.* **10** L537